Original Article

Estimation of Postmortem Interval by Light and Electron Microscopic Findings in the Liver of Adult Male Albino Rats

Ola Abdel Hady Sweilum [1], Amira A. M. Fouda [2], Fatma Shaban Kandeel[3].

1,3 Forensic Medicine and Clinical Toxicology Department, Faculty of Medicine- Menoufia University, Egypt. 2- Pathology Department, Faculty of Medicine - Menoufia University, Egypt.

ABSTRACT

Corresponding author:

Ola Abdel Hady Sweilum

Email:
olaahady@hotmail.com

Mobile: 01019898260

Background: Estimating the postmortem interval (PMI) is one of the most challenging tasks and difficult, longstanding problems in forensic practice from ancient times up to the present. Post-mortem interval is paramount in daily forensic casework, as it can help with the identification of human remains and assist in death investigations**.** The light microscope remains the most important tool for the study of cell microstructures by using a light beam. Electron microscope (EM) is a powerful sensitive technique for tissue imaging, that is used for estimating PMI. EM uses a beam of electrons instead of a light beam. **Objectives**: The aim of the study is to estimate the post-mortem interval (PMI) in experimental adult male albino rats by studying the histological changes in the liver using light and transmission electron microscope (TEM) techniques. **Methods**: Thirty male albino rats were randomly divided into six groups (five rats each). All rats (30 rats) were sacrificed by cervical dislocation at the same time. The liver was obtained from each rat group at different PM time points as follow: group 1 (Control group): at the moment of death. Group 2: half-hour PMI. Group 3: one-hour PMI. Group 4: two hours PMI. Group 5: four hours PMI. Group 6: six hours PMI. **Results**: results are obtained by light and electron microscopic examinations. The light microscopic changes were observed as early as 30 minutes since death, whereas ultra-structurally significant difference in morphology was observed in more detailed from 30 minutes and increased in time dependent manner till complete homogenization at 6 hours interval. **Conclusion**: Light and electron microscopic findings of the liver tissue sample were found to be helpful in establishing the post-mortem interval.

Key words:

Forensic practice; postmortem interval; Electron Microscope, Light microscope.

1- INTRODUCTION:

Estimating the postmortem interval (PMI) is one of the most challenging tasks and difficult, longstanding problems in forensic practice from ancient times up to the present (Henssge and Madea, 2004). PMI is determined as the length of time that has passed between the occurrence of death and the discovery of the dead body (El-Harouny et al., 2008). It helps investigators to reconstruct the circumstances in the case of a suspicious death or homicide. (Young et al., 2013)

Postmortem interval (PMI) is paramount in daily forensic casework, as it can help with the identification of human remains and assists in death investigations (Cockle and Bell, 2015)**.** It is not only important in criminal cases or violent deaths but also, in civil cases such as insurance and inheritance (Sachdeva et al., 2011, Salam H. 2012**;** Shrestha et al., 2021)**.**

The body undergoes complex and sophisticated natural changes after death. A sequence of unavoidable and irreversible physical and chemical changes begins immediately in the body following death. These changes are subjected to great variability due to wide environmental and circumstantial effects (Brooks, 2016).

Individual factors, such as age and sex, also have a strong influence on PMI estimations (Ali, 2017). Environmental factors must also be taken into consideration in calculating the PMI, such as temperature, exposure to rainfall, humidity, depth and composition of the burial place, and insect activity (Mann et al., 1990).

There are various methods used to detect the PMI, including physical changes (lividity, cooling), bacterial effect (putrefaction), entomological study, physicochemical (rigor mortis), and biochemical changes (Sara et al., 2014). Recently genetic (DNA and RNA) application has been done aiming at a more accurate PMI estimation (Bévalot et al., 2015; Hilal, 2017).

The light microscope remains the most important tool for studying cell microstructures by using a light beam. Light microscopes can be used as a primary visualization tool for PM changes or in support of electron microscopy (Light Microscopy Subject Guide 2013).

Electron microscope (EM) is a powerful sensitive technique for tissue imaging, that is used for estimating PMI. EM uses a beam of electrons instead of a light beam. This allows for higher magnification, higher resolving

power, and thus more accurate cell details. During PMI, Ultrastructure changes appear early as the tissues are degraded by autolytic processes (Sarah, 2020). Electron microscopy allows studying bacterial ultrastructure at high resolutions (Hammerschmidt and Rohde, 2019).

The present study aimed to estimate the post-mortem interval (PMI) in experimental adult male albino rats by studying the histological changes in the liver using light and transmission electron microscope (TEM) techniques.

II- MATERIALS AND METHODS:

*Animal:

Thirty adults male Wistar albino rats (weighing 230-260 grams; 12 weeks old) were purchased from an animal house in Shebin El Kom City, Menoufia, Egypt.

Rats were housed in polypropylene cages. The animals were given one week to get acclimatized to the condition of the laboratory before starting the experiment. They were maintained on a 12-h light/dark cycle, at 28°c temperature and air humidity of 40%, with free access to food and water.

*Experimental design:

This experiment was carried out in the animal laboratory in the Faculty of Medicine, Menoufia University, Egypt.

Thirty male albino rats were randomly divided into six groups (five rats each). All rats (30 rats) were sacrificed by cervical dislocation, and the liver was obtained from each rat at the time determined in the following groups:

- Group 1 (Control group): at the moment of death.
- Group 2: half-hour PMI.
- Group 3: one-hour PMI.
- Group 4: two hours PMI.
- Group 5: four hours PMI.
- Group 6: six hours PMI.

All experimental groups were left under the same environmental condition during the period between the time of death and liver removal.

The liver was removed, washed with saline, and prepared for histological study. The tissues were prepared for light microscopic examination with hematoxylin & eosin (H&E) (Kiernan 2015). and for ultrastructure examination using electron microscopy.

* Histological specimens' preparation:

Light microscope:

Specimens from the liver were fixed in 10% buffered formalin at a temperature of 4°C. Tissue samples were dehydrated in ascending grades of alcohol (50%, 70%, 90% overnight, and 100% for 3 hours), cleared in xylol, and embedded in paraffin. Tissue sections (5 μm thickness) were stained with hematoxylin & eosin (H &E) (Bancroft & Gamble 2008).

Electron microscope:

Specimens for electron microscopy were fixed immediately in 2.5% phosphate-buffered glutaraldehyde (pH 7.4). Then, they were post-fixed in 1% osmium tetroxide in the same buffer at 4°C, dehydrated, and embedded in epoxy resin. Ultrathin sections were stained with uranyl acetate and lead citrate and examined and photographed using a JEOL JEM 1010 electron microscope (Jeol Ltd, Tokyo, Japan) in the Electron Microscope Research Laboratory of the Histology and Cell Biology Department, Faculty of Medicine, Tanta University (Egypt), and in the JEOL JEM 1200 EXII Electron Microscope (Jeol Ltd) Research Laboratory, Faculty of Medicine, Tanta University, Egypt (Glauert & Lewis 1998).

Morphometric analysis:

It included the measuring of:

- Nucleus diameter in H&E-stained sections at a magnification of x400.

- Diameter of the nucleus in EM sections at a magnification of x1500.
- Diameter of mitochondria in EM sections at a magnification of x1500.

An average diameter was calculated by computing the geometric mean of the maximum and minimum diameters as the nuclei and the mitochondria were generally non-circular. Results from 50 randomly selected cells were averaged to determine the mean transverse diameter. All measurements were done in 10 nonoverlapping randomly chosen fields for each animal. Image analysis was done using ″ (Image J-Image Processing 1.74v; National Institute of Health, Bethesda, Maryland, USA).

Statistical analysis:

Data were fed to the computer and analyzed using IBM SPSS software version 20.0. (Armonk, NY: IBM Corp). The Kolmogorov- Smirnov was used to verify the normality of variables'; comparisons between groups for categorical variables were assessed using the Chi-square test (Fisher). Judged Significance of the obtained results was at the 5% level.

III- RESULTS:

Light and electron microscopes revealed considerable changes.

Light microscopic results:

Examination of H&E-stained sections of the rat liver after death showed:

The control group (group 1) shows normal hepatic tissue (aligned hepatocytes with distinct sinusoids). The lobular architecture is preserved although with visible congestion, and edema. (Figure 1). Sections of group 2 (30 minutes after death) shows a slightly disrupted hepatic tissue with homogenization and eosinophilia, the nucleus showed chromatin condensation. (Figure 2). Sections of group 3 (one hour after death) shows disrupted hepatic tissue with loss of cell membrane and increased homogenization and eosinophilia, with Nuclear karyorrhexis, visible hemorrhage, congestion, and edema also appears. (Figure 3)

Sections of group 4 (two hours after death) shows more eosinophilia and sparce cytoplasmic vacuolization, and disturbed lobular architecture compared with the other groups; increased karyorrhexis of the nucleus with announcing karyolysis (Figure 4). Sections of group 5 (four hours after death) shows more eosinophilia and increasing cytoplasmic vacuolization compared with the previous groups. Nuclear changes are in the form of more pyknosis, increased karyorrhexis with increasing karyolysis. (Figure 5)

Sections of group 6 (six hours after death) shows eosinophilia, overwhelming nuclear changes including pyknosis, karyorrhexis and karyolysis Progressing to complete disappearance in some cells (Figure 6).

Electron Microscopic results:

Examination of rat liver sections by electron microscope showed:

Control group: Hepatocyte has nucleus with prominent nucleolus. The cytoplasm shows many mitochondria with some cisternae of rough endoplasmic reticulum. (Figure 7; a, b)

After 30 minutes of death: Mitochondria is swollen; Endoplasmic reticulum (ER) shows beadlike enlargement, inconsistent detachment of ribosomes. The Nucleus has a regular nuclear membrane and evenly distributed euchromatin and occasional clumped heterochromatin. The Mitochondria (m) and Rough Endoplasmic Reticulum (RER) are normally distributed and reveal no morphological alterations. (Figure 8; a, b, c)

EM liver Changes after one hour: clumping of the nuclear chromatin and irregular nuclear membrane. There is dilation of rough endoplasmic reticulum around the nucleus. The mitochondria show swelling,

loss of cristae. cytoplasm shows small vacuoles (Figure 9; a, b, c).

EM Changes after two hours are in the form of severely swollen mitochondria, disappearance of cristae and interruption of mitochondrial membrane. nucleus shows clumping of chromatin, marked swelling of the ER (endoplasmic reticulum) compared with one hour finding. Cytoplasm shows enlargement with more vacuoles compared with one hour findings. (Figure 10; a, b)

After 4 hours of death, the EM shows cytoplasmic vacuoles and lysis of the mitochondria with other organelles. The nucleus shows Karyolysis, granularity and irregular nuclear membrane (Figure 11; a, b, c, d). EM Changes after 6 hours are in the form of marked destruction (haemogenization) of cell organelles mainly mitochondria with lysis of their inner cristae and appearance of many vacuoles. ER shows lysis. Part of nucleus appears showing Karyolysis and irregular nuclear membrane. Cytoplasm also shows marked vacuolation. (Figure 12; a, b, c, d, e, f).

Morphometric analysis results:

Regarding the mitochondrial diameter changes in different studied groups, table 1 shows significant increases in mitochondrial diameter (by EM) corresponding to the postmortem time in the first four studied groups, with the greatest increase in group IV (2 hours after death) (Mean± SD: 2.01 ± 0.08) then the diameter significantly decreases in the last two groups (V and VI) (table 1).

Table 2 shows significant increases in the nuclear diameter (by EM) corresponding to the postmortem time in the first four studied groups, with the greatest increase in group IV (2 hours after death) (mean ±SD: 10.44 ± 0.35) then the diameter significantly decreases in the last two groups.

Table 3 shows the nuclear diameter changes by light microscope, there is a significant increase in the nuclear diameter that corresponds to the postmortem time in the first four studied groups, with the greatest increase in group IV (2 hours after death) (Mean ± SD: 7.68 ± 0.26), then the diameter significantly decreases in the last two groups.
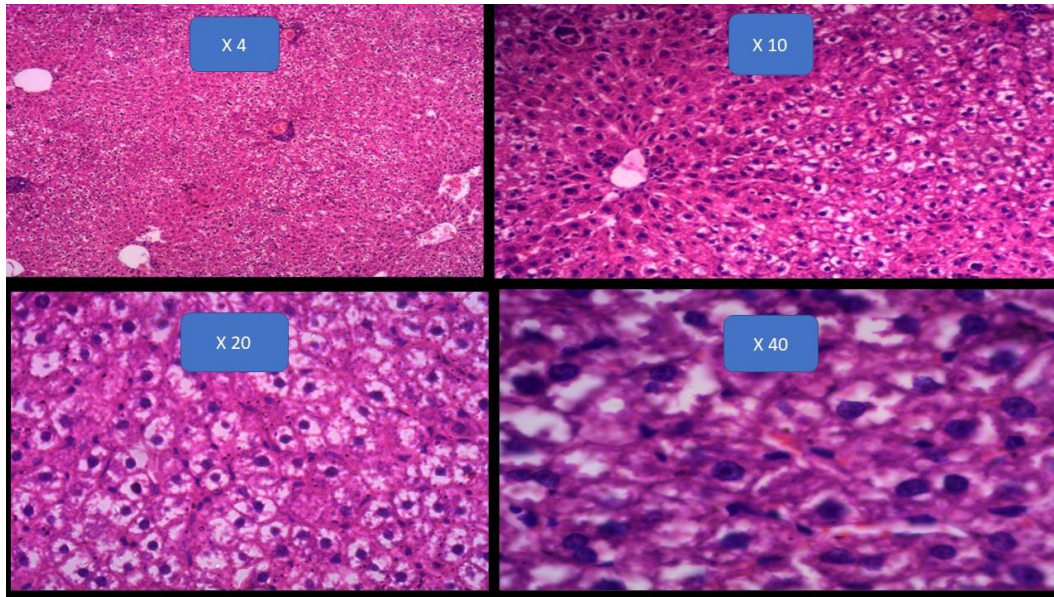
Figure 1: Control group (at the time of death): A photomicrograph in a section of male albino rat liver by light microscope shows a normal hepatic tissue (aligned hepatocytes with distinct sinusoids). The lobular architecture is preserved. H. & E. stain x400.
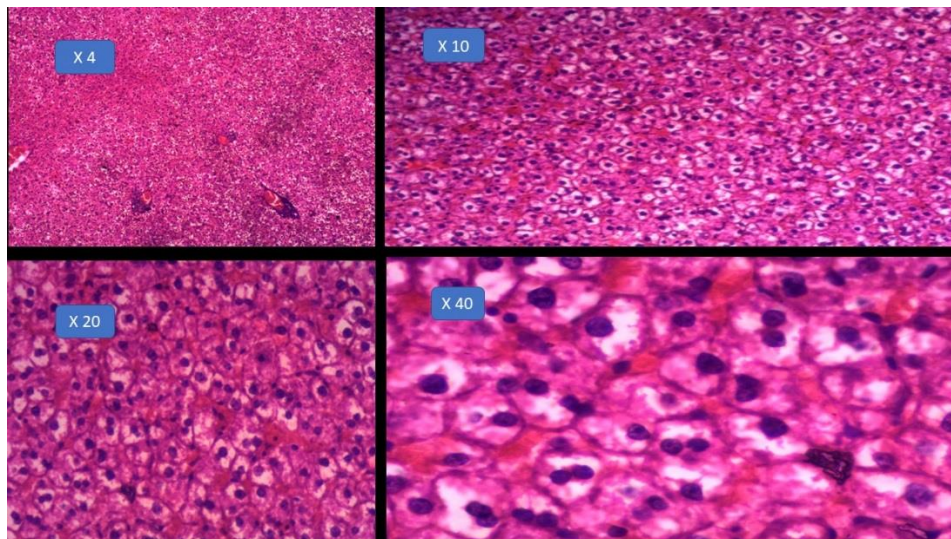

Figure 2: 30 minutes after death (group 2): A photomicrograph in a section of male albino rat liver by light microscope shows a slightly disrupted hepatic tissue with homogenization and eosinophilia. Sparce nuclear changes show chromatin condensation. H. & E. stain x400.
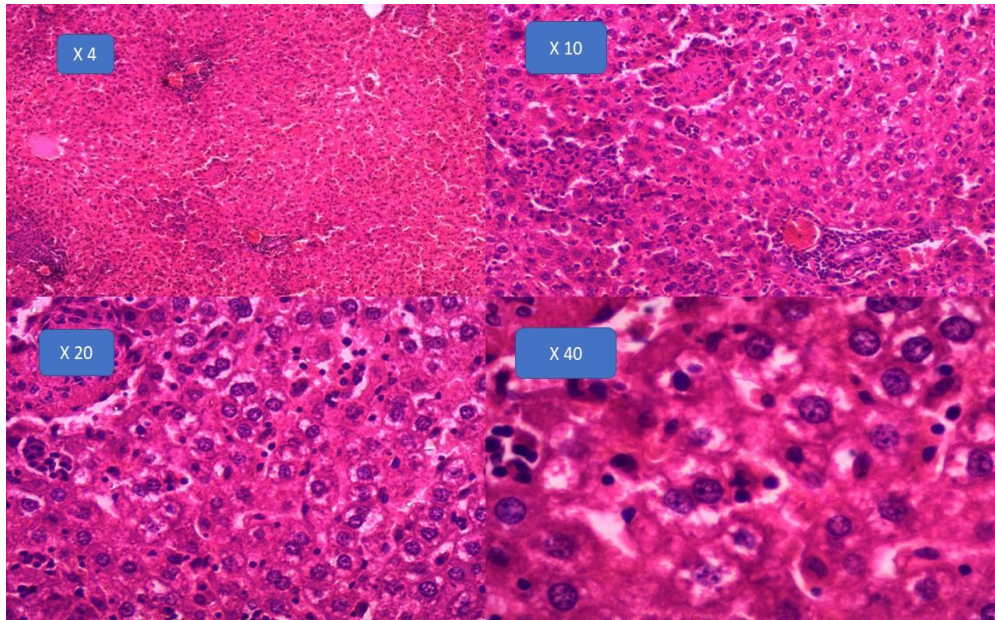
Figure 3: One Hour after death (group 3): A photomicrograph in a section of male albino rat liver by light microscope shows disrupted hepatic tissue with loss of cell membrane with increased homogenization and eosinophilia. Nuclear changes show karyorrhexis. Visible hemorrhage, congestion, and edema. H. & E. stain x400.
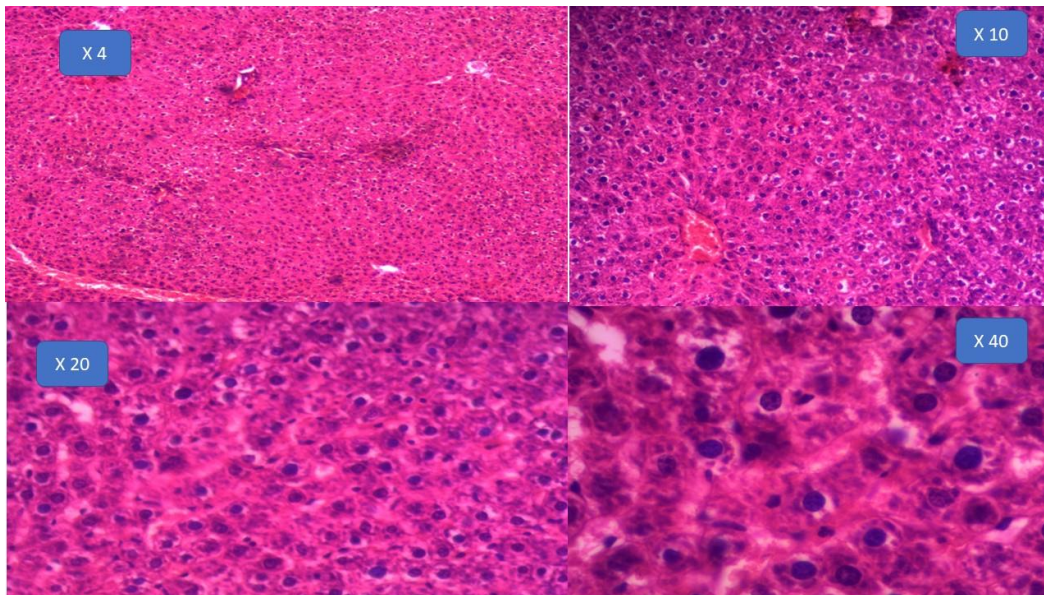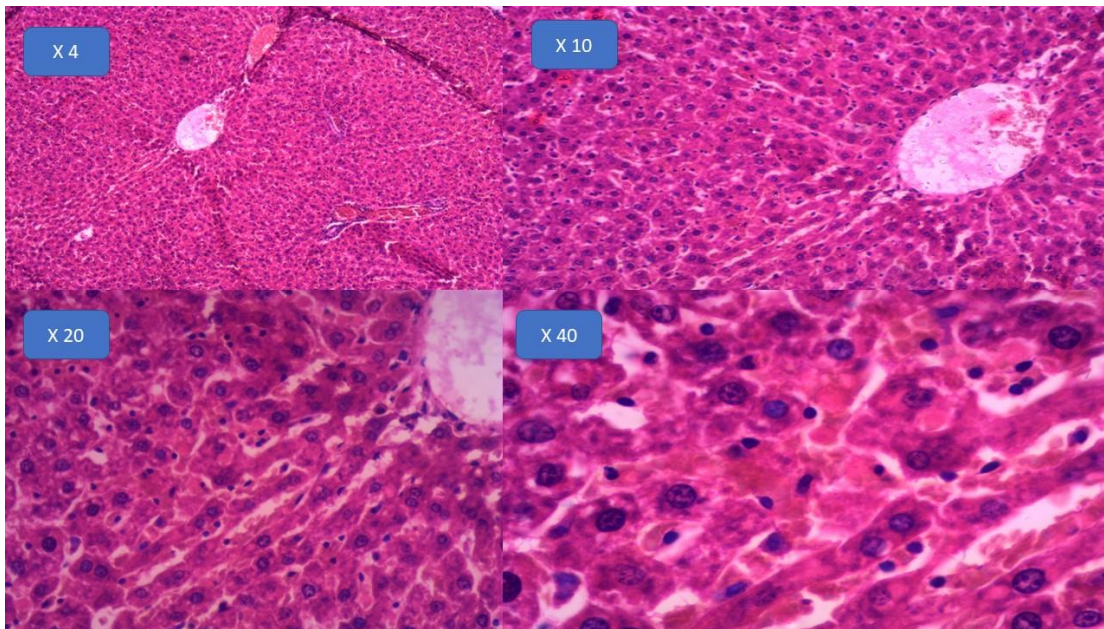

Figure 4: Two hours after death (group 4): A photomicrograph in a section of male albino rat liver by light microscope shows disturbed lobular architecture. More eosinophilia and sparce cytoplasmic vacuolization. Nuclear changes show increased karyorrhexis with announcing karyolysis. H. & E. stain x400.
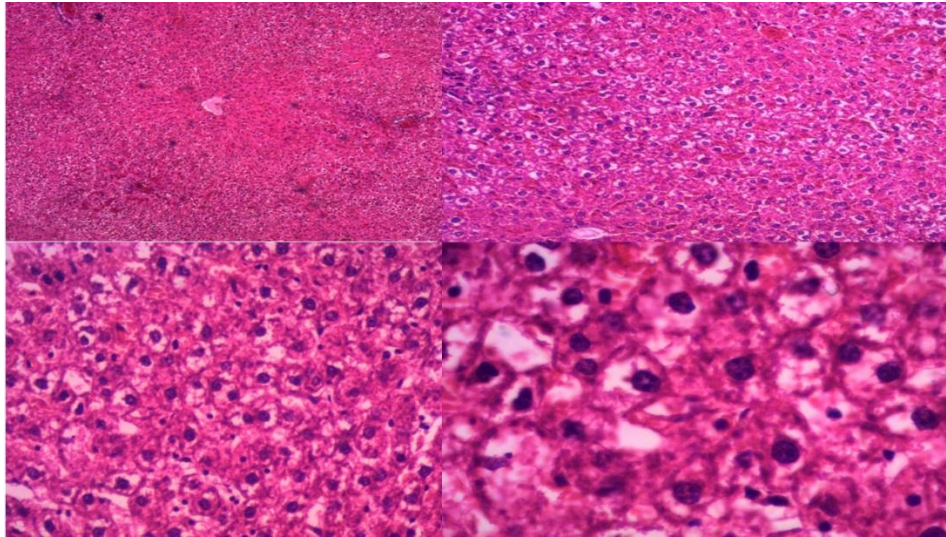
Figure 5: Four hours of death (group 5): A photomicrograph in a section of male albino rat liver by light microscope shows more eosinophilia and increasing cytoplasmic vacuolization. Nuclear changes show more pyknosis, and increased karyorrhexis with increasing karyolysis. H. & E. stain x400.


Figure 6: Six hours after death (group 6): A photomicrograph in a section of male albino rat liver by light microscope shows eosinophilia. Pyknosis, karyorrhexis and karyolysis. Multiple foci of necrotic cells. H. & E. stain x400.
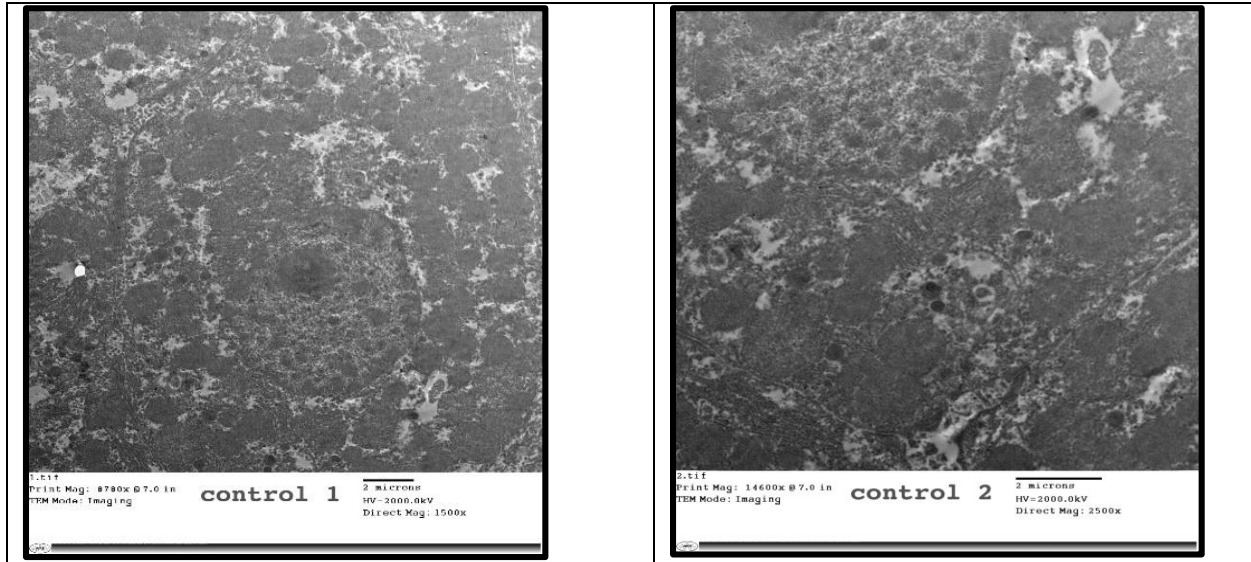
Figure 7: Transmission electron micrograph of rat hepatocyte in **control** group: Hepatocyte has nucleus with prominent nucleolus. The cytoplasm shows many mitochondria with some cisternae of rough endoplasmic reticulum.
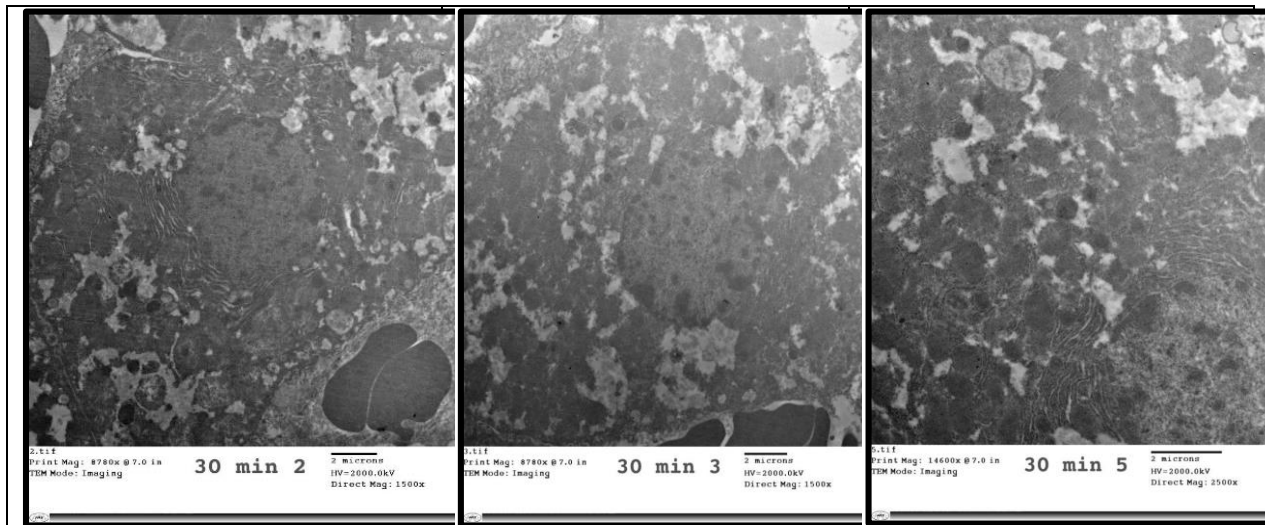
Figure 8: Transmission electron micrograph of rat hepatocyte after **30 minutes** of death (group 2): Mitochondrial swelling; Endoplasmic reticulum (ER) shows beadlike enlargement, inconsistent detachment of ribosomes. The nucleus has a regular nuclear membrane. The Mitochondria and Rough Endoplasmic Reticulum (RER) are normally distributed.
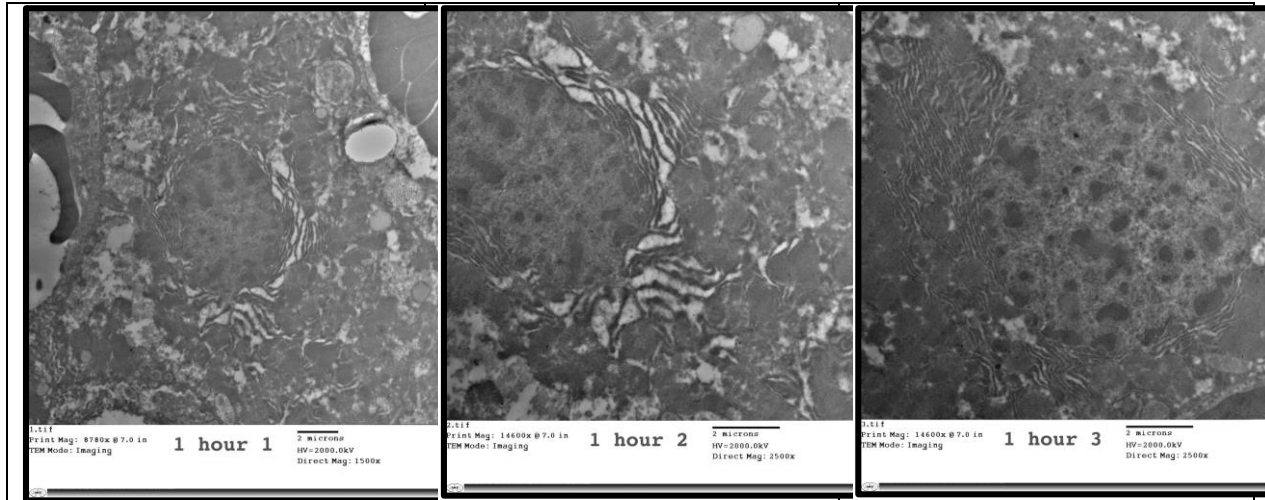
Figure 9: Transmission electron micrograph of rat hepatocyte one hour after death (group 3): The nucleus shows clumpin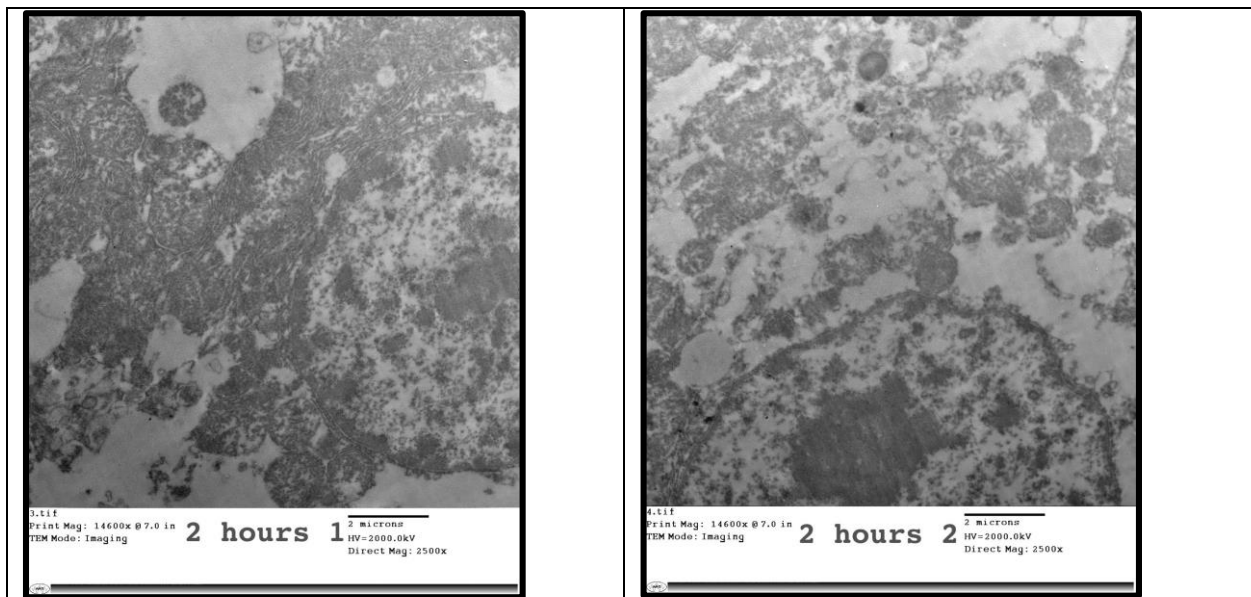g of chromatin and irregular nuclear membrane. There is dilatation (swelling) of RER around the nucleus. The mitochondria show more swelling, and loss of cristae. Cytoplasm shows small vacuoles.

Figure 10: Transmission electron micrograph of rat hepatocyte two hours after death (group 4): Mitochondria is severely swollen, with the disappearance of cristae and interruption of the mitochondrial membrane. Nucleus shows clumping of chromatin with nuclear membrane detachment. ER shows marked swelling. Cytoplasm shows enlargement with vacuoles.
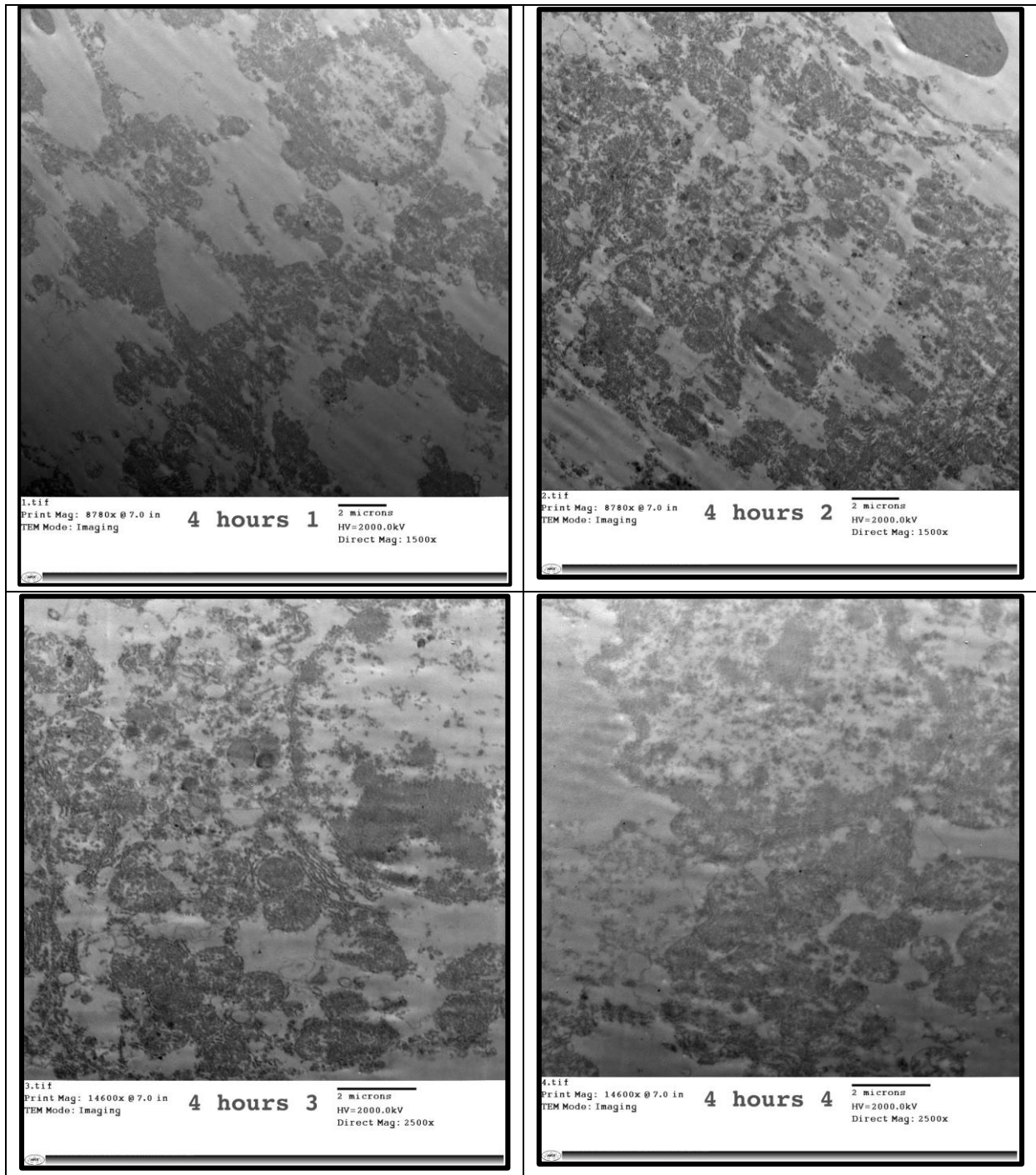
Figure 11: Transmission electron micrograph of rat hepatocyte 4 hours after death (group 5): There are cytoplasmic vacuoles. Mitochondria with other organelles show lysis. The nucleus shows karyolysis, granularity, and irregular nuclear membrane.
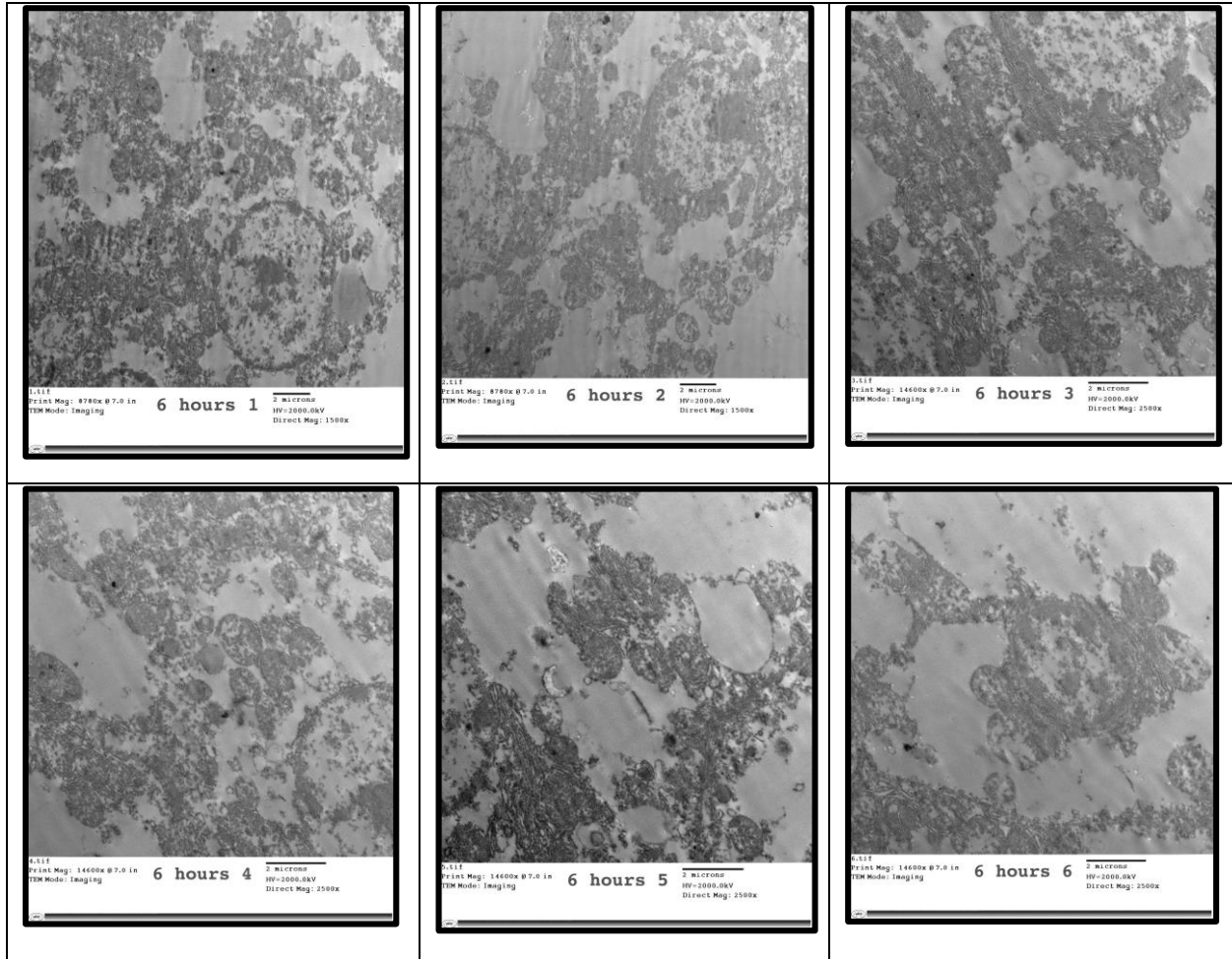
Figure 12: Transmission electron micrograph of rat hepatocyte 6 hours after death (group 6): Part of the cytoplasm of hepatocyte showing marked vacuoles and homogenization of cell organelles, mainly the mitochondria with lysis of their inner cristae and appearance of many vacuoles. ER shows lysis. Part of nucleus appears to show Karyolysis and, irregular nuclear membrane & leakage of chromatin.

Table 1: Mitochondrial diameter changes in the different studied groups by Electron Microscope by one-way Anova test.

Mitochondrial diameter	Group I	Group II	Group III	Group IV	Group V	Group VI	F test	P value
mean±SD	1.41±0.06	1.73±0.10	1.83±0.10	**2.01±0.08**	1.64±0.06	1.44±0.06	87.62	0.001
Range	1.29-1.5	1.55-1.89	1.69-1.98	1.95-2.2	1.56-1.76	1.35-1.55		
P1		0.001	0.001	0.001	0.001	0.353		
P2			0.005	0.001	0.01	0.001		
P3				0.001	0.001	0.001		
P4					0.001	0.001		
P5						0.001		

P1 comparison regard Group I   P2 comparison regard Group II

P3 comparison regard Group III   P4 comparison regard Group IV   P5 comparison regard Group V

Table 2: Nuclear diameter changes in different studied groups by Electron Microscope (one-way Anova test).

Nucleus diameter EM	Group I	Group II	Group III	Group IV	Group V	Group VI	F test	P value
Mean±SD	7.69±0.26	6.62±0.08	6.14±0.11	10.44±0.35	9.73±0.55	6.85±0.23	332.17	0.001
Range	6.99-7.88	6.49-6.73	5.99-6.32	9.99-11.01	9.02-10.55	6.41-7.13		
P1		0.001	0.001	0.001	0.001	0.001		
P2			0.001	0.001	0.001	0.106		
P3				0.001	0.001	0.001		
P4					0.001	0.001		
P5						0.001		

P1 comparison regard Group I   P2 comparison regard Group II

P3 comparison regard Group III   P4 comparison regard Group IV   P5 comparison regard Group V

Table 3: Nuclear diameter changes in different studied groups by Light microscope using one-way Anova test.

Nuclear diameter by LM.	Group I	Group II	Group III	Group IV	Group V	Group VI	F test	P value
Mean±SD	5.96±0.18	6.47±0.18	7.08±0.10	7.68±0.26	7.19±0.06	6.70±0.23	108.25	0.001
Range	5.75-6.31	6.21-6.71	6.97-7.23	7.32-8.11	7.11-7.32	6.52-7.13		
P1		0.001	0.001	0.001	0.001	0.001		
P2			0.001	0.001	0.001	0.008		
P3				0.001	0.191	0.001		
P4					0.001	0.001		
P5						0.001		

P1 comparison regard Group I   P2 comparison regard Group II

P3 comparison regard Group III   P4 comparison regard Group IV   P5 comparison regard Group V

IV- DISCUSION:

Estimating the postmortem interval (PMI) is crucial in human death investigations. It allows the retrospective estimation of the time of death (Brooks 2016).

The use of decomposition alone to estimate the post-mortem interval is discouraged, so Examining changes in the ultrastructure is an important method for determining the PMI. (Gelderman et al.,2019)

After death, anoxic post-mortem effects are known to cause alterations in enzyme activity and ultrastructural cells (Majno and Joris, 1995). Changes in shape, size, and

localization of cell structures are all part of the autolytic process, which results in the gradual loss of highly organized structural organization of cells (Van Cruchten and Van Den Broeck, 2002). The occurrence of autolysis is quick in tissues which have a high concentration of autolytic enzymes, such as the liver (Scarpelli and Iannaccone, 1990).

The current study examined the post-mortem alterations in rat liver samples using light and electron microscopes.

Regarding light microscopic changes in rat liver in the present study, rat hepatocytes showed early changes that began 30 minutes after death. These early changes were in the

form of eosinophilia and sparse nuclear changes that is result in protein coagulation.

These changes increased over time as after one hour, there were disturbances in the hepatic tissue with loss of cell membrane, increased homogenization, and eosinophilia. Karyorrhexis can be seen in nuclear alterations. Hemorrhage, congestion, and edema were all visible.

While 2 hours after death in our study, disturbed lobular architecture and cytoplasmic vacuoles started to appear. Eosinophilia increased, and nuclear karyorrhexis increased with announcing karyolysis.

In the current study, changes after 4 hours of death, were eosinophilia and cytoplasmic vacuolization that increased compared with the previous PM intervals, increased nuclear karyorrhexis with karyolysis and pyknosis.

Overwhelming nuclear changes progressed to complete disappearance in some cells, and multiple necrotic cell foci appeared after 6 hours of death.

These findings are in agreement with the study of Kimura and Abe who observed a reduced stainability of erythrocytes, atrophy of hepatocytes, sinusoidal dilatation and karyopyknosis of endothelial or Kupffer cells, swelling of nuclei and karyopyknosis with an evident eosinophilic cytoplasm at the male rat liver at body temperature after 3-5 hours of death (Kimura and Abe, 1994).

Yamamoto et al., reported autolytic alterations, shrinkage of hepatocytes, and disruption of hepatic chords in human individuals, as well as a wavy transformation of hepatocytes, in a post-mortem investigation (Yamamoto et al., 1997).

Supriya Das, et al. (2019) found that the goat liver specimens collected at 12-hours after death showed nuclear condensation and increased granularity of cytoplasm in the hepatocytes.

Wenzlow et al. (2021) discovered that in the first 72 hours after death, PM histological alterations in horses were most predicted in the liver and muscle. Hepatocyte individualization and separation of the bile duct epithelium from the basement membrane, high eosinophilia, and loss of striation were all evident as autolysis criteria. The present study demonstrated that the light microscopic changes occurred during the early postmortem period, in contrast Janssen et al., who reported that it was difficult to identify postmortem changes by light microscopy (Janssen et al.,1984).

Regarding the electron microscopic (EM) findings, the alterations in the PM ultrastructure in the liver tissue after half an hour were mitochondria swelling (because of increased membrane permeability) as well as progressive fragmentation of cristae and ribosomal detachment. These changes are similar to that observed by Tomitaa et al., who reported cell swelling, dense amorphous deposits in the mitochondria, loss of glycogen granules, dilation of the endoplasmic reticulum (ER), clumping, and margination of nuclear chromatin (Tomitaa et al., 2004). While Li et al., (2003) observed hepatocyte vacuoles in male rats immediately after death.

Postmortem electron microscopic changes in the present study after one-hour were in the form of clumping of chromatin of the nucleus and irregular nuclear membrane, dilation of rough endoplasmic reticulum, and swelling of the mitochondria.

Tomitaa et al., (2004) observed EM changes after one hour of death, in the form of cell edema (cell swelling), clumping of nuclear chromatin, and the loss of mitochondrial cristae were seen in the hepatocytes; the degree of mitochondrial cristae loss increased with time, these changes were the same in the first 10 hours after death.

In the current study, at 2 hours after death, the PM electron microscopic changes were: mitochondria were severely swollen with the disappearance of cristae, interruption of its membrane, vacuoles. Endoplasmic reticulum more pronounced compared to one hour, cytoplasm enlarged, and nucleus shows granulation and chromatin clumping.

These changes are correlated with that observed by Slauson and Cooper, who reported swollen organelles, including the mitochondria and endoplasmic reticulum, started to rupture from 2 to 4 hours after death (Slauson and Cooper, 2000).

Karadžić et al., (2010) observed similar hepatocyte changes after 2 hours of death, in the form of chromatin granulation and clumping, fragmentation of mitochondrial cristae, marked swelling of ER, and golgi apparatus membrane.

In accordance with the study done by Muthukrishnan et al., (2018) on the gingival tissue, who observed mitochondrial swelling in both 2 and 4 h of post-mortem and were numerous in 2 h PMI tissue when compared to 4 h since death. Disruption of mitochondrial membrane and altered shape of mitochondria was evident in 4 h postmortem gingival tissue.

According to the present study, an EM shows changes after 4 hours postmortem in the form

of cytoplasmic vacuoles. Lysis of the mitochondria and other organelles. karyolysis, the granularity of the nucleus with the irregular nuclear membrane. These results are similar to the study findings by Kuypers and Roomans during the same PM interval (Kuypers and Roomans, 1980)

Karadžić et al. (2010), observed hepatocytic changes in the form of outer nuclear membrane lysis, initial vacuolization of sarcoplasm (at 4 hours after death).

While Kuypers & Roomans indicated that no significant mitochondrial volume increase compared to two hours (Kuypers and Roomans, 1980).

In the present study, at 6 hours after death, EM showed marked destruction (homogenization) of cell organelles, mainly the mitochondria. Lysis of ER. Part of nuclear Karyolysis and irregular nuclear membrane.

Similar changes at 6 hours after death were observed by Karadžić et al., (2010) including lysis of the inner nuclear membrane with consequent leakage of chromatin in sarcoplasm, significant loss of mitochondrial cristae, moderate vacuolization of sarcoplasm, decrease in the number of glycogen granules.

The reported variations in the postmortem intervals were likely associated with animal species, strain, sex, and/or study conditions.

V- CONCLUSION:

Light and electron microscopic findings of the liver tissue sample were found to be useful in establishing the postmortem interval.

It had been established that ultrastructural changes of hepatocytes are conditioned by the duration of post-mortal time (time-dependent). So, properly detecting the ultrastructure changes is useful for estimating the postmortem interval.

Ultrastructure changes appear early, so it is helpful in determining the early postmortem interval.

Initial post-mortem changes are in the mitochondrial structures of liver tissue, while significant nuclear changes in the hepatocyte were generally observed later than homogenization of the tissue appeared after 6 hours.

VI- Recommendations:

*Using ultrastructure for estimating the PMI in further studies is a useful, applicable method in early PM periods.

*Further studies are needed at variable temperatures and humidity; it also needs to

be done under different pathological conditions.

VII-ETHICAL CONSIDERATIONS:

The experimental protocol was approved by the Menoufia University Research Ethics Committee (NO. 5/2022FORE5).

VIII- Conflicts of interest: There are no conflicts of interest.

IX- REFERENCES:

- **Ali, M.M.; Ibrahim, S.F. and Fayed, A.A. (2017):** Using Skin Gene Markers for Estimating Early Postmortem Interval at Different Temperatures. Am J Forensic Med Pathol. Dec;38(4):323-325.

- **Bancroft, J.D. and Gamble M. (2008):** Theory and practice of histological techniques. 6th Edition, Philadelphia, PA: Churchill Livingstone; Elsevier, China.

- **Bévalot, F.; Cartiser, N.; Bottinelli, C.; Fanton, L. and Guitton. J. (2015):** Vitreous humor analysis for the detection of xenobiotics in forensic toxicology: a review. Forensic toxico.; 34, 12–40**.**

- **Brooks, J. W. (2016):** Postmortem Changes in Animal Carcasses and Estimation of the Postmortem Interval. Vet. Path. J., 53(5) 929-940.

- **Cockle, D.L. and Bell, L.S. (2015):** Human decomposition and the reliability of a 'Universal' model for postmortem interval estimations. Forensic Sci Int.; 253:136: e1–136.

- **El-Harouny, M.A.; El-Dakroory S.A.; Attalla S.M.; Hasan N. A.; and Hassab El-Nabi S. E. (2008):** The Relationship Between Postmortem Interval and DNA Degradation in Different Tissues of Drowned Rats. Mansoura j. forensic med. clin. toxicology. Vol. XVI, No. 2.

- **Gelderman, H.T.; Kruiver, C.A.; Oostra, R.J.; Zeegers, M.P.; Duijst, W.L. (2019):** Estimation of the postmortem interval based on the human decomposition process. J Forensic Leg Med; 61:122-127.

- **Glauert, A.M. and Lewis, P.R. (1998):** Biological specimen preparation for transmission electron microscopy. 1st ed. London: Portland Press.

- **Hammerschmidt, S. and Rohde, M. (2019):** Electron Microscopy to Study the Fine Structure of the Pneumococcal Cell. Methods Mol Biol; 1968:13-33.

- **Henssge, C. and Madea, B. (2004):** Estimation of the time since death in the early post-mortem period. Forensic Sci Int. Sep 10;144(2-3):167-75.

- **Hilal, M. A.; El-sayed, W.A.; Said, A. M.; and Magdy, A. (2017):** Updates in Estimating Postmortem Interval Sohage medical journal. 21 (3):171-174.

- **Janssen, W. (1984):** Forensic histopathology. Berlin: Springer; p. 15–47.

- **Karadžić, R.; Ilić, G.; Antović, A. and Banović, L.K. (2010):** Autolytic ultrastructural changes in rat and human hepatocytes. Rom J Leg Med, 18(4):247–252.

- **Kiernan, J.A. (2015):** Histological and histochemical methods; theory and practice. 5th ed. Oxford, UK: Butterworth Heinemann; 238–300. Scion Publishing Ltd, Banbury, UK ISBN 978 1 907904 32 5: 571.

- **Kimura, M. and Abe, M. (1994):** Histology of postmortem changes in rat livers to ascertain hour of death. Int J Tissue React ;16(3):139-50.

- **Kuypers, G.A.J. and Roomans, G.M. (1980):** Postmortem elemental redistribution in rat studied by X-ray microanalysis and electron microscopy. Histochemistry; 69(2):145–156.

- **Li, X.; Elwell, M.R.; Ryan, A.M. and Ochoa, R. (2003):** Morphogenesis of postmortem hepatocyte vacuolation and liver weight increases in Sprague-Dawley rats. Texico. Pathol.; 31(6):682-8.

- **Light Microscopy Subject Guide. Metallogr. Microstruct. Anal. 2, 48–52 (2013).** https://doi.org/10.1007/s13632-012-0059-z.

- **Majno, G. and Joris, I. (1995):** Apoptosis, oncosis, and necrosis - an overview of cell death. Am. J. Pathol.; 146(1):3-13.).

- **Mann, R.W., Bass, W.M., and Meadows, L. (1990):** Time since death and decomposition of the human body: variables and observations in case and experimental field studies. J Forensic Sci;35(1):103-11.

- **Muthukrishnan, S.; Narasimhan, M.; Paranthaman, SK.; Hari, T.; Viswanathan, P. and Rajan, S.T. (2018):** Estimation of time since death based on light microscopic, electron microscopic, and electrolyte

analysis in the gingival human tissue. J Forensic Dent Sci;10(1):34-39.

- **Sachdeva, N.; Rani, Y.; Singh, R. and Murari, A. (2011):** Estimation of postmortem interval from the changes in vitreous biochemistry. J Indian Acad. Forensic Med.; 33:171–4.

- **Salam, H.; Shaat, E.; Aziz, M.; Moneim Sheta, A. and Hussein, H. (2012):** Estimation of postmortem interval using thanatochemistry and postmortem changes. Alex J Med.; 48:335–44.

- **Sarah, M. (2020):** The Determination of Post-Mortem Interval (PMI) Using Transmission Electron Microscopy. Azo. Life Sciences. From https://www.azolifesciences.com/article/The-Determination-of-PMI-Using-Electron-Microscopy.aspx.

- **Scarpelli, D.G. and Iannaccone, P.M. (1990):** Cell death, autolysis and necrosis. In: Kissane JM, editor. Anderson's pathology. 9th ed. St. Louis: Mosby:13.

- **Shrestha, R., Kanchan, T., and Krishan, K. (2021):** Methods of Estimation of Time Since Death. In:

Stat Pearls [Internet]. Treasure Island (FL): www.statpearls.com Publishing.

- **Slauson, D.O. and Cooper, B.J. (2000):** Mechanisms of disease: A textbook of comparative general pathology, No.Ed.3 pp. 45–53.

- **Supriya, Das., S.K.; Panda, A.P.; Acharya, U.K.; Mishra, A.K.; Kundu, B.N. and Ali, I. (2019):** Postmortem Blood and Tissue Changes for Estimation of Time of Death. Int.J.Curr.Microbiol.App.Sci. 8(09): 43-53.

- **Tomitaa, Y.; Nihiraa, M.; Ohnoa, Y. and Satob, S. (2004):** Ultrastructural changes during in situ early postmortem autolysis in kidney, pancreas, liver, heart and skeletal muscle of rats.N: Leg. Med.; 6:25–31.

- **Van Cruchten, S. and Van Den Broeck, W. (2002):** Morphological and biochemical aspects of apoptosis, oncosis and necrosis. Anat Histol Embryol. Aug;31(4):214-23.

- **Wenzlow, N.; Neal, D.; Stern, AW. and Prakoso, D. (2021):** Feasibility of using tissue autolysis to estimate the postmortem interval in horses. J. of vet. Diag. invests., 33 (5): 825-833.

- **Yamamoto, K.; Yamamoto, Y.; Matsumoto, H.; Hayase, T.; Ojima, K.; Matsubayashi, K.; Abiru, H. and Kazuko, K. (1997):** Unusual post-mortem autolytic change in the liver: the wavy transformation of hepatocytes. Medical Science Law, 37(3): 256-9.

- **Young, S.T.; Wells, J.D.; Hobbs, G.R. and Bishop, C.P. (2013):** Estimating postmortem interval using RNA degradation and morphological changes in the tooth pulp. Forensic Sci. Int., 229: 163.e1–163.e6.

- **Zapico, C. S.; Menéndez, S.T., and Núñez, P. (2014):** Cell death proteins as markers of early postmortem interval. Mol. Life Sci;71(15):2957-62.

الملخص العربي

تقدير الفترة الزمنية بعد الوفاة بالميكروسكوب الضوئي و الإلكتروني في كبد ذكور الفئران البيضاء البالغة

علا عبد الهادي منصور[1] أميرة فوده[2] فاطمة شعبان قنديل[3]

1,3قسم الطب الشرعي والسموم الاكلينيكية -كلية الطب ـ جامعة المنوفية

2 قسم الباثولوجيا – كلية الطب ـ جامعة المنوفية

يعد تقدير فترة ما بعد الوفاة أحد أصعب المهام والمشكلات الطويلة الأمد في ممارسة الطب الشرعي من العصور القديمة وحتى الوقت الحاضر. وهو يعد أمرًا بالغ الأهمية في أعمال الطب الشرعي اليومية، حيث يمكن أن يساعد في تحديد هوية الرفات البشرية ويساعد في التحقيقات المتعلقة بالوفاة.

يخضع الجسم لسلسلة من التغيرات الفيزيائية والكيميائية التي لا رجعة فيها وتبدأ على الفور في الجسم بعد الوفاة. والتي تتأثر بالعوامل البيئية مثل درجة الحرارة، وهطول الأمطار، والرطوبة، وعمق مكان الدفن وتكوينه، ونشاط الحشرات وغيرها

يظل المجهر الضوئي أهم أداة لدراسة الهياكل المجهرية للخلية باستخدام شعاع ضوئي. بينما المجهر الإلكتروني فهو يستخدم تقنية حساسة قوية لتصوير الأنسجة بدقه حيث يستخدم حزمة من الإلكترونات بدلاً من شعاع الضوء.

الهدف من هذه الدراسة هو تقدير فترة ما بعد الوفاة في ذكور الجرذان البيضاء التجريبية البالغة من خلال دراسة التغيرات النسيجية في الكبد باستخدام تقنيات المجهر الضوئي والالكتروني.

الطريقة:

تم تقسيم ثلاثين من ذكور الجرذان البيضاء بشكل عشوائي إلى ست مجموعات (خمسة جرذان لكل مجموعة). تم موت الجرذان بخلع العنق في نفس الوقت. تم الحصول على الكبد من كل مجموعة جرذان في نقاط زمنية مختلفة على النحو التالي:

• المجموعة الأولى (المجموعة الضابطة): لحظة الوفاة.

• المجموعة 2: بعد الوفاة بنصف ساعة.

• المجموعة 3: بعد الوفاة بساعة واحدة.

• المجموعة 4: بعد الوفاة بساعتين.

• المجموعة 5: بعد الوفاة بأربع ساعات.

• المجموعة 6: بعد الوفاة بست ساعات

تم الحصول على النتائج عن طريق الفحص المجهري الضوئي والإلكتروني. وقد لوحظت التغييرات الميكروسكوبية الضوئية في وقت مبكر من نصف ساعة بعد الوفاة، في حين لوحظت تغيرات كثير' بشكل أكثر تفصيلاً بالميكروسكوب الالكتروني من نصف ساعة وزاد بطريقة تعتمد على الوقت حتى حدوث تغير كامل للتفاصيل الداخلية للخلية عند 6 ساعات.

التوصيات:

يوصي باستخدام التغيرات الميكروسكوبية لتقدير زمن الوفاه في مزيد من الدراسات حيث انه طريقة مفيدة وقابلة للتطبيق في تحديد الفترات المبكرة بعد الوفاة.

* هناك حاجة إلى مزيد من الدراسات في درجات حرارة ورطوبة متغيرة؛ كما يجب القيام به في ظل ظروف مرضية مختلفة.